

High resolution 3D ^{31}P spectroscopic imaging of the human prostate at 7T: technical feasibility and *in vivo* measurement

T. Kobus¹, A. K. Bitz², M. J. Van Uden¹, M. W. Lagemaat¹, S. Orzada², A. Heerschap¹, and T. W. Scheenen^{1,2}

¹Radiology, Radboud University Nijmegen Medical Centre, Nijmegen, Gelderland, Netherlands, ²Erwin L. Hahn Institute for Magnetic Resonance Imaging, Essen, Germany

Introduction:

Some key phosphorylated metabolites can be observed by ^{31}P MR spectroscopy. Previous application to the prostate detected different metabolite levels in cancer tissue. In these studies an endorectal coil was used to obtain a single unlocalized spectrum at low field (2T) in 10-30 minutes (1-2). A much better SNR is expected at 7T, enabling localized 3D ^{31}P spectroscopic imaging. To this end, anatomical imaging is necessary to relate the metabolic information to location. For prostate imaging at 7T one could use a 8-channel ^1H TxRx array coil, combined with B1^+ shimming methods (3). In this work we present SAR safety measurements of a combined ^{31}P TxRx endorectal and 8-channel ^1H array coil together with 3D ^{31}P MRSI of the prostate and surrounding tissues with adiabatic excitation. For safe use, the maximum power deposition of the ^{31}P endorectal coil itself and the coupling between the elements of the 8-channel ^1H coil and the ^{31}P endorectal coil need to be known. Due to the wavelengths of the ^1H frequency in biological tissues at 7T, the ^{31}P prostate coil and cables might interfere with the 8-channel ^1H array coil, which could lead to increased flip angles or power deposition. In this study we dealt with the prerequisites for a safe and feasible setup that combines an 8-channel ^1H array coil with an endorectal ^{31}P coil and showed *in vivo* results of proton MRI and ^{31}P MRSI with optimized adiabatic excitation.

Methods:

All measurements were performed on a 7T whole body MR system (Magnetom, Siemens, Erlangen). For the ^{31}P endorectal coil the mechanical housing and conductors of an inflatable 3T endorectal coil (Medrad, USA) were adapted (Fig 1A). The coil was tuned and matched to 50Ω at 120.3 MHz. For imaging, a home build 8-channel ^1H TxRx array system was used with meander elements (4), and home build B1^+ shimming and SAR supervision software and systems were used (5). On a phantom MR thermometry was used to determine the temperature increase after 5min40sec of RF deposition of 5.6W with the ^{31}P coil. To confirm the phantom B1^+ and heat distributions, Finite Integration Technique (FIT) calculations of a detailed human prostate model were performed to assure compliance with safety guidelines. Gel phantom measurements ($\epsilon_r=45$ and $\sigma=0.8$ S/m) with the endorectal coil and 8-channel array coil were also used to study possible coupling between the two coils. 47W of RF power was transmitted for 2 minutes with the 8-channel ^1H array coil, after which MR thermometry was performed. A B1^+ map was acquired to study changes in the RF field distribution of the 8-channel ^1H array coil due to the presence of the ^{31}P endorectal coil. After all safety validations and maximum power assessments, a healthy volunteer was examined. Following fast gradient echo localizers and B1^+ shimming of the 8 individual elements for maximal phase coherence, T2w imaging of three slices in 1.5 minutes was performed (TE 71 ms TR 3 s). A pulse acquire sequence with an adiabatic BIR 4 pulse of 45 degrees for excitation was used for 3D ^{31}P MRSI of the full field of view of the endorectal coil. The acquisition bandwidth was set to 5000 Hz and the TR was 1500ms. In two different acquisitions with different

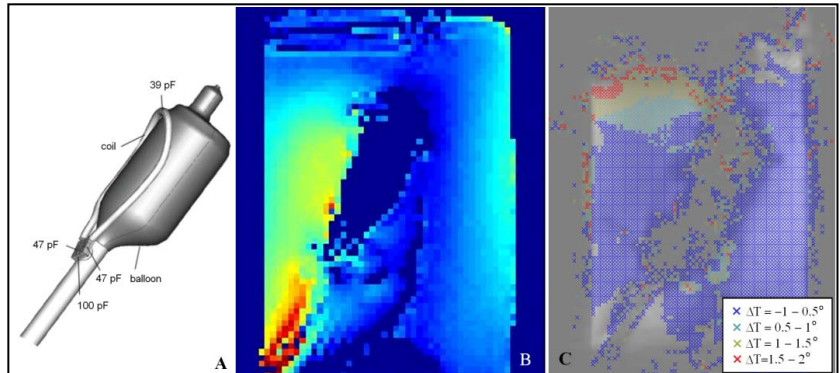


Fig 1. A: The ^{31}P TxRx endorectal coil on an inflatable balloon. B: The B1^+ distribution in a phantom while sending with the 8 channel ^1H TxRx coil. C: The temperature map after transmitting 47W of RF power for 2 minutes with the 8 channel ^1H TxRx coil.

spatial resolution (5.8 cc voxels after apodization of weighted k-space sampling in 11 minutes and 4.0 cc voxels in 18 minutes) high-quality ^{31}P spectra were acquired from the prostate, bladder, seminal vesicles and surrounding muscles.

Results:

A maximum temperature increase of 3°C was observed in the gel phantom close to the capacitors after RF deposition of 5.6W with the ^{31}P coil. This corresponds to a safe power deposition of 1.8W for 6 minutes for a 1°C increase in temperature. There was a slightly larger temperature increase observed at the feeding point of the coil, which was confirmed by the FIT model (Fig 2). Fig. 1B shows the B1^+ distribution of the 8 channel ^1H coil in the presence of the endorectal coil. An increased flip angle is observed near the cable of the coil. However, this increased B1 field did not result in increased temperature as shown in Fig 1C. Therefore, the ^{31}P endorectal coil has no influence on the SAR limits of the 8 channel ^1H coil. The use of the 8-channel ^1H array coil with B1^+ shimming gave good imaging results of the prostate as shown in Fig 3A, which is necessary to relate spectra to location. The resonances of phosphocholine (PC), phosphoethanolamine (PE), inorganic phosphate (Pi), phosphocreatine (PCr) and γ -, α - and β -phosphates of ATP are clearly visible. The intensity of the β -phosphate was attenuated due to the limited bandwidth of the adiabatic pulses. A metabolite map of the fitted integral of the PCr signal was made using the high resolution ^{31}P MRSI with the 4 cc voxels. This image illustrates adequate localization of larger PCr signals (Fig. 3C) in muscles around the prostate and lower PCr signal intensity in the prostate itself.

Conclusion and Discussion:

Although some very preliminary initial results of using a ^{31}P endorectal coil at 7T were reported earlier (6), we demonstrated with this work that it is safe and feasible to combine a 8 channel ^1H TxRx coil with a TxRx endorectal ^{31}P coil for *in vivo* prostate imaging and ^{31}P MRSI. With adiabatic excitation individual metabolites of PE, PC, PCr, Pi and the γ -, α - and β -phosphates were visible with a relatively high spatial resolution throughout the prostate and surrounding tissues, showing the potential of ^{31}P MRSI of the prostate at high field.

References: [1] Kurhanewicz, MRM (1991) 22:404; [2] Thomas, J Magn Reson (1992) 99:377; [3] Metzger, MRM (2008) 59:396 [4] Orzada ISMRM 2999 (2009); [5] Bitz ISMRM (2009) 4767; [6] Arteaga ISMRM (2010) 2805; **Acknowledgement:** Dutch Cancer Society KUN 2007/3971, ERC Grant agreement n^o [243115]

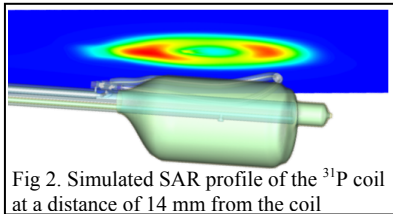


Fig 2. Simulated SAR profile of the ^{31}P coil at a distance of 14 mm from the coil

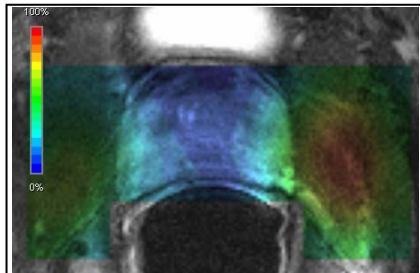


Fig 4. PCr metabolite overlay high resolution ^{31}P MRSI with 4 cc voxels.

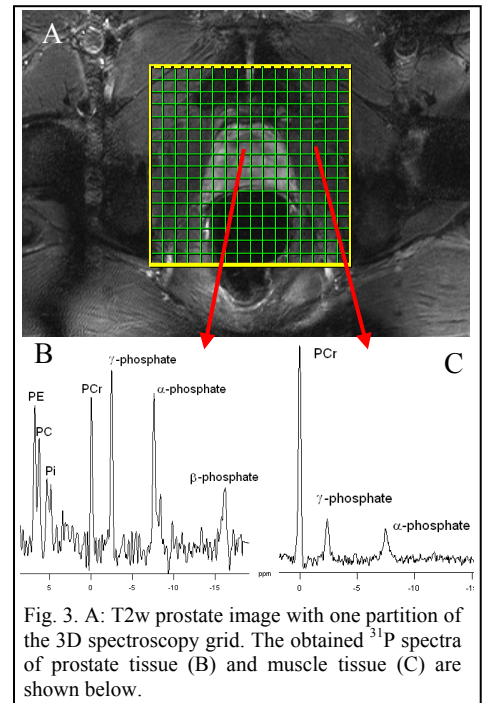


Fig 3. A: T2w prostate image with one partition of the 3D spectroscopy grid. The obtained ^{31}P spectra of prostate tissue (B) and muscle tissue (C) are shown below.